Generalized One-Band Model Based on Zhang-Rice Singlets for Tetragonal CuO

I. J. Hamad and L. O. Manuel
Instituto de Física Rosario (CONICET) and Universidad Nacional de Rosario, Boulevard 27 de Febrero 210 bis, 2000 Rosario, Argentina

A. A. Aligia*
Centro Atómico Bariloche and Instituto Balseiro, CNEA, CONICET, 8400 Bariloche, Argentina

(Received 31 October 2017; published 27 April 2018)

Tetragonal CuO (T-CuO) has attracted attention because of its structure similar to that of the cuprates. It has been recently proposed as a compound whose study can give an end to the long debate about the proper microscopic modeling for cuprates. In this work, we rigorously derive an effective one-band generalized $t-J$ model for T-CuO, based on orthogonalized Zhang-Rice singlets, and make an estimative calculation of its parameters, based on previous *ab initio* calculations. By means of the self-consistent Born approximation, we then evaluate the spectral function and the quasiparticle dispersion for a single hole doped in antiferromagnetically ordered half filled T-CuO. Our predictions show very good agreement with angle-resolved photoemission spectra and with theoretical multiband results. We conclude that a generalized $t-J$ model remains the minimal Hamiltonian for a correct description of single-hole dynamics in cuprates.

DOI: 10.1103/PhysRevLett.120.177001

More than three decades after their discovery, high-temperature superconductors still give rise to many debates. On the theoretical side, one of the most long-standing and important discussions is about the proper microscopic model for describing superconductivity. In this respect and from the outset, attention was focused on the spectral function of a single hole doped on the parent half filled compounds, whose quasiparticle (QP) dispersion relation is directly measured in angle-resolved photoemission (ARPES) experiments. Experimental evidence shows that this doped hole resides on the O $2p_\sigma$ orbitals [1–3]. For the CuO_2 planes that build up the cuprates, Zhang and Rice [4] proposed that a singlet, called the Zhang-Rice (ZR) singlet, is formed between the spin of a copper atom and the spin of the hole residing in a linear combination of four ligand oxygen orbitals around the copper atom. Integrating out the oxygen orbitals, a one-band effective model was proposed in which the effective holes (representing ZR singlets) reside on the copper atoms and propagate emitting spin excitations, magnons. In this model, adding two holes as nearest neighbors in an antiferromagnetic background costs less energy than if they are added far apart. This is a simplified view of the pairing glue of magnetic origin [5].

Since the proposal of Zhang and Rice, an unclosed debate about the validity of one-band effective models has taken place [6–16]. Several authors sustain that only the three-band model [17,18] is valid for describing the physics of the cuprates correctly, where the three bands come from two O $2p_\sigma$ orbitals and one Cu $3d_{x^2-y^2}$ orbital, not only for the insulating parent compound at half filling but also for many other phases of the rich phase diagram of the cuprates and related compounds. This issue is of central importance, since many investigations have been done in one-band models, and hence their validity is, at least partially, questioned.

Recently, tetragonal CuO (T-CuO) has been synthesized, by growing epitaxially CuO planes on a substrate [(001) $SrTiO_3$] [19]. T-CuO can be considered as two interpenetrating CuO_2 sublattices sharing one oxygen atom and hence has two degenerate antiferromagnetic ground states, as shown in Fig. 1. ARPES experiments were performed on this compound [20], showing substantial intralayer coupling between these two sublattices and a similar dispersion (with some differences) to that of the cuprate $Sr_2CuO_2Cl_2$. This material was addressed in a recent work [15] as a good candidate to discern whether one-band models, based on ZR singlets, are valid for describing the physics of CuO planes or if, instead, three-band models should be used.

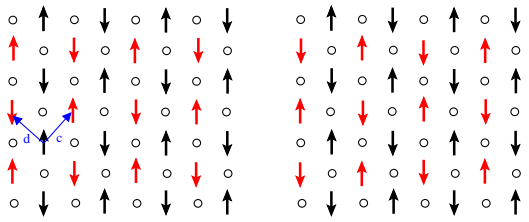

FIG. 1. The two possible magnetic ground states for T-CuO: $\mathbf{Q} = (0, \pi)$ (left) and $\mathbf{Q} = (\pi, 0)$ (right). The coordinate versors point in the directions of **c** and **d**. Arrows indicate spins at Cu sites, and circles correspond to the O sites.

In this Letter, we rigorously derive an effective one-band model for T-CuO and compare its QP dispersion with experimental ARPES results and theoretical predictions for the three-band model. Using a procedure based on previous derivations of generalized one-band effective Hamiltonians [10], we start from a spin-fermion model for T-CuO, and we obtain then its effective one-band model for the ZR singlets. The parameters of the model were calculated starting from parameters determined by constrained-density-functional computations for La_2CuO_4 [21] and estimating their variations for the T-CuO case. We find an effective hopping to first nearest neighbors (NN) between CuO_2 sublattices and effective hoppings to first, second, and third NN in the same sublattice, together with superexchange parameters J (the usual NN antiferromagnetic one for CuO_2 planes) and a ferromagnetic J' (NN in T-CuO, belonging to different CuO_2 sublattices).

Using this model, we calculate the QP dispersion by means of the self-consistent Born approximation (SCBA), a reliable and widely used many-body method. We compare our results with ARPES experiments in T-CuO, obtaining good qualitative and quantitative agreements. Our results also recover previous ones from a three-band calculation, including particular aspects that were claimed absent in a ZR picture. We then conclude that our method is correct for obtaining rigorous one-band effective models and that the one-band model that we have derived describes correctly the physics of a single doped hole in T-CuO.

We start from a spin-fermion model (Cu spins and O holes), obtained by integrating out valence fluctuations at the Cu sites [6,15,22–24]. With the adequate choice of phases (Fig. S1 in Ref. [24]), the Hamiltonian reads

$$\begin{aligned} H_{sf} = & \sum_{i\delta\delta'\sigma} p^{\dagger}_{i+\delta'\sigma} p_{i+\delta\sigma} \left[(t_1^{sf} + t_2^{sf}) \left(\frac{1}{2} + 2\mathbf{S}_i \cdot \mathbf{s}_{i+\delta} \right) - t_2^{sf} \right] \\ & - J_d \sum_{i\delta} \mathbf{S}_i \cdot \mathbf{s}_{i+\delta} + \frac{J}{2} \sum_{i\delta} \mathbf{S}_i \cdot \mathbf{S}_{i+2\delta} \\ & - t_{pp} \sum_{j\gamma\sigma} p^{\dagger}_{j+\gamma\sigma} p_{j\sigma} + t'_{pp} \sum_{j\gamma\sigma} s_{\gamma} (p^{\dagger}_{j+\gamma\sigma} p_{j\sigma} + \text{H.c.}) \\ & - \frac{J'}{2} \sum_{i\gamma} \mathbf{S}_i \cdot \mathbf{S}_{i+\gamma}, \end{aligned} \tag{1}$$

where i (j) labels the Cu (O) sites and $i+\delta$ ($j+\gamma$) label the four O atoms nearest to Cu atom i (O atom j). The spin at the Cu site i (O orbital $2p_\sigma$ at site $i+\delta$) is denoted as $\mathbf{S}_i$ ($\mathbf{s}_{i+\delta}$). The signs $s_\gamma = -1$ for $\gamma \| \hat{\mathbf{x}} + \hat{\mathbf{y}}$ and $s_\gamma = 1$ in the perpendicular direction, $\hat{\mathbf{x}}$ and $\hat{\mathbf{y}}$ being the unit vectors along the directions of NN Cu atoms in the CuO_2 planes (which are second NN in the T-CuO structure). The parameter $t'_{pp} \simeq 0.6 t_{pp}$ (Ref. [15]). This is essentially the same Hamiltonian as that considered by Adolphs *et al.* [15] (we include virtual fluctuations via Cu^{+3}), and its low-energy physics reproduces that of the three-band model [23].

Projecting the Hamiltonian over the subspace of orthogonal ZR singlets, we have derived a one-band generalized $t-J$ model for T-CuO. All the steps can be found in Ref. [24]. The one-band effective generalized $t-J$ Hamiltonian is

$$\begin{aligned} H^s_{tJ} = & -\sum_{\kappa=0}^{3} t_\kappa \sum_{i v_\kappa \sigma} (c^{\dagger}_{i\sigma} c_{i+v_\kappa\sigma} + \text{H.c.}) \\ & + \frac{J}{2} \sum_{i v_1} \mathbf{S}_i \cdot \mathbf{S}_{i+v_1} - \frac{J'}{2} \sum_{i v_0} \mathbf{S}_i \cdot \mathbf{S}_{i+v_0}, \end{aligned} \tag{2}$$

where the subscript $\kappa = 0$ refers to intersublattice hopping of NN Cu atoms in the T-CuO structure, while $\kappa = 1, 2, 3$ refer to first, second, and third NN within each CuO_2 sublattice, respectively. Instead of using arbitrary values for the parameters, we have calculated them, keeping the states corresponding to orthogonalized ZR singlets and using results from constrained-density-functional calculations [21]. These values are very similar to those corresponding to the model used by Adolphs *et al.* [15], as shown in Table 3 in Ref. [24]. We have checked that the results for both sets are quite similar. To simplify the discussion, we present here only the results for the latter. The parameters in meV are $t_0 = -184$, $t_1 = 369$, $t_2 = -11$, $t_3 = 65$, $J = 150$, and $J' = 0$. This effective model was proposed previously by Moser *et al.* [20]. Here we provide its justification and determine its parameters.

The spectral functions were calculated by means of the SCBA [36–39], a semianalytic method that has been proven to compare very well with exact diagonalization (ED) results on finite clusters in different systems [36,37,39–41]. It is one of the more reliable and checked methods up to date to calculate the hole Green's function and, in particular, its QP dispersion relation. However, some care is needed to map the QP weight between different models [37]. In order to do such calculation, we follow standard procedures [36]. On one hand, the magnetic dispersion relation is obtained by treating the magnetic part of the Hamiltonian at the linear spin-wave level, since the system we study has long-range order, and hence its magnetic excitations are semiclassical magnons. On the other hand, the electron creation and annihilation operators in the hopping terms are mapped into holons of a slave-fermion representation (details in Ref. [24]). Within SCBA, we arrive to an effective Hamiltonian:

$$\begin{aligned} H_{\text{eff}} = & \sum_{\mathbf{k}} \epsilon_{\mathbf{k}} h^{\dagger}_{\mathbf{k}} h_{\mathbf{k}} + \sum_{\mathbf{k}} \omega_{\mathbf{k}} \theta^{\dagger}_{\mathbf{k}} \theta_{\mathbf{k}} \\ & + \frac{1}{\sqrt{N}} \sum_{\mathbf{kq}} (M_{\mathbf{kq}} h^{\dagger}_{\mathbf{k}} h_{\mathbf{k}-\mathbf{q}} \theta_{\mathbf{q}} + \text{H.c.}), \end{aligned} \tag{3}$$

$$\epsilon_{\mathbf{k}} = 2t_0\cos(\mathbf{k}\cdot\mathbf{c}) + 4t_2\cos(ak_x)\cos(ak_y) + 2t_3[\cos(2ak_x)+\cos(2ak_y)],$$
$$\omega_{\mathbf{k}} = \sqrt{A_{\mathbf{k}}^2 - 4B_{\mathbf{k}}^2},$$
$$M_{\mathbf{kq}} = 2t_0\{\cos[(\mathbf{k}-\mathbf{q})\cdot\mathbf{c}]u_{\mathbf{q}} - \cos(\mathbf{k}\cdot\mathbf{c})v_{\mathbf{q}}\} + 2t_1[u_{\mathbf{q}}\zeta(\mathbf{k}-\mathbf{q}) - v_{\mathbf{q}}\zeta(\mathbf{k})], \quad (4)$$

where $\epsilon_{\mathbf{k}}$ is the bare hole dispersion (with no coupling to magnons), $\omega_{\mathbf{k}}$ is the magnon dispersion relation, with $A_{\mathbf{k}} = 2J - J'\cos(\mathbf{c}\cdot\mathbf{k})$ and $B_{\mathbf{k}} = (J/4)\sum_{v_1}\cos(v_1\cdot\mathbf{k}) - (J'/2)\cos(\mathbf{d}\cdot\mathbf{k})$, and $M_{\mathbf{kq}}$ is the vertex that couples the hole with magnons. Here $\zeta(\mathbf{k}) = \cos(ak_x)+\cos(ak_y)$, $\mathbf{c} = b(\hat{\mathbf{x}}+\hat{\mathbf{y}})$, and $\mathbf{d} = b(-\hat{\mathbf{x}}+\hat{\mathbf{y}})$, $a = 2b$ being the distance between Cu atoms in the CuO_2 planes. The vectors $\mathbf{c}$ and $\mathbf{d}$ are indicated in Fig. 1. We now compare our results with ARPES experiments performed on T-CuO, specifically with those in Figs. 2 and 3 in Ref. [20]. For that purpose, we adopt in Figs. 2 and 3 an electron picture. In Fig. 2, we show the QP dispersion derived from our SCBA calculation. This should be compared with the blue points in Fig. 2 in Ref. [20] and also with the white points in the same figure, corresponding to exact diagonalization of a one-band Hubbard model in 20 sites. In our calculation, a broadening equivalent to 20 meV [controlled by means of the parameter δ in Eq. (4)], similar to the experimental resolution (30 meV [20]), was applied to the spectral functions. Taking into account the two possible magnetic ground states for T-CuO, we obtain the two QP dispersions shown in Fig. 2. It can be observed that the dispersion corresponding to $\mathbf{Q} = (\pi, 0)$ recovers all the main features of the experimental dispersion, and hence our results can distinguish between the possible degenerate magnetic orders in the experiment. In particular, we recover the asymmetry between the points Γ and X', B and B', and A and A'. Moreover, we obtain $E(A) - E(A') = 128$ meV, $E(B) - E(B') = 64$ meV, and $E(\Gamma) - E(M) = 10$ meV, while the experimentally measured energy differences are 140, 60, and 180 meV, respectively [20]. The agreement is very good, except in the last case. This discrepancy is quite likely due to missing quasiparticle peaks with small weight in the experiment (see also Fig. S4 in Ref. [24]). In that sense, we note that the Γ point (and points located in its vicinity) shows a very broad spectrum (see Figs. 2 and 3 in Ref. [20]), and hence there may be some uncertainty in the determination of the QP energy which could explain this discrepancy. The bandwidth of the QP dispersion, along this path, taken from our SCBA calculation is 0.3 eV, very similar to the bandwidth of the experimental dispersion, approximately 0.4 eV. We have also calculated an intensity curve along the same path as in the experiment, to compare with the ARPES intensities (Fig. 2 in Ref. [20]). We show only the intensity corresponding to $\mathbf{Q} = (\pi, 0)$, since for this order our QP dispersion recovers the experimental one. For this calculation, a broadening equivalent to 170 meV was applied, in order to make the intensity plot softer. The results are shown in Fig. 3. The similarities with the experimental curve follow the trends explained in the previous paragraph. It is worth mentioning that, on one hand, at some points in the experimental curve the effect of the ARPES matrix elements is very strong, especially around the X/M' point, where there is no intensity at all in the ARPES data, and, on the other hand, a β band seems to merge with the QP band, especially at the X/M' point but also possibly around the M point. So at these two points, in particular, around the X/M' points, the comparison of our calculation with the experiment is obscured by these experimental facts. Finally, it is worth mentioning that, in the case that the illuminated area in the ARPES experiments contains domains with both magnetic $\mathbf{Q} = (\pi, 0)$ and $\mathbf{Q} = (0, \pi)$ vectors (as mentioned above, they are degenerate), the QP dispersion should be a superposition of both curves shown in Fig. 2, which does not seem to be what is observed in the experiment [42]. The intensity

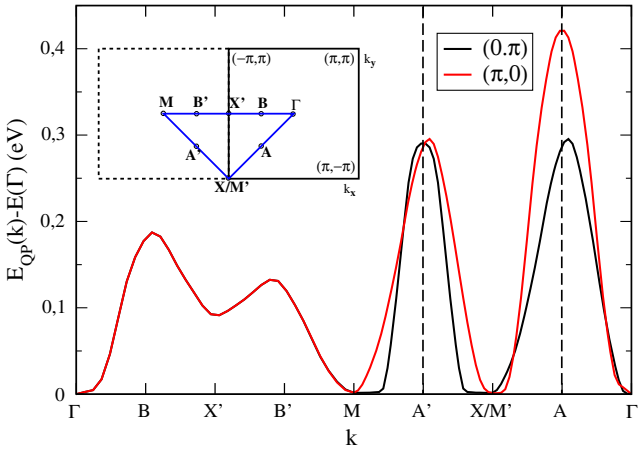

FIG. 2. Quasiparticle dispersion relation (relative to Γ) along the path marked in the inset, the same as the one measured in the ARPES experiment in Ref. [20]. A broadening equivalent to 20 meV was applied to the spectral functions (see the text).

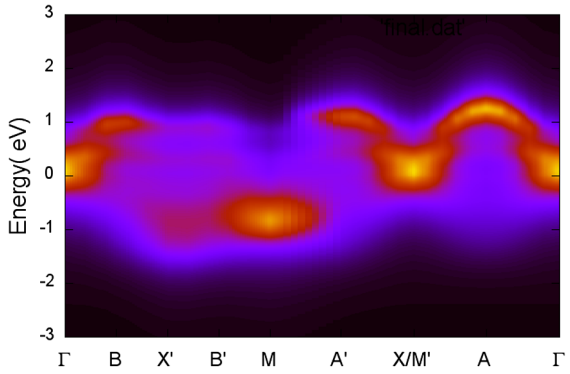

FIG. 3. SCBA intensity map along the same path as in Fig. 2. The assumed magnetic order is $(\pi, 0)$.

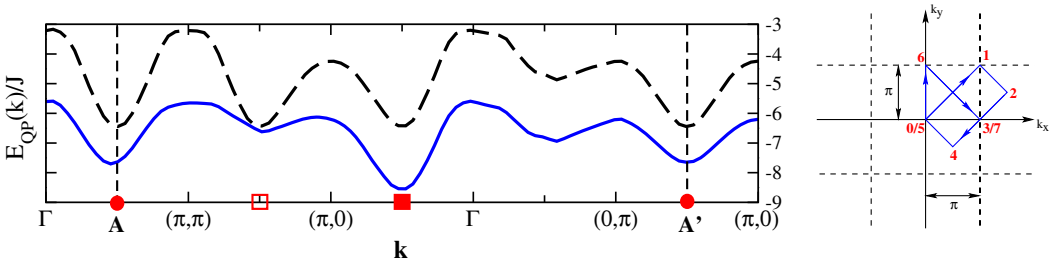

FIG. 4. SCBA hole dispersion relation in units of J (0.15 eV) along the path marked in the inset. Black dashed line: The result corresponding to $t_0 = 0$ (decoupled sublattices). Blue full line: The full result with $t_0 = -184$ meV.

curve in Fig. 3 should also change accordingly, but in our case we have checked that the only noticeable changes occur around the X/M' point, at which nevertheless there is no intensity in the ARPES data corresponding to the band ascribed to ZR singlets [20].

In general, the spectral function corresponding to a definite momentum contains, in the hole picture, a low-energy pole, whose energy defines the QP energy, and a high-energy part which is related to the incoherent movement of the hole, having its origin in multimagnon processes [40]. When the quasiparticle weight is significant, the brighter areas in Fig. 3 will coincide with the energy of the QP in Fig. 2. On the contrary, when the incoherent part of the spectral function takes most of the spectral weight, this will not happen. Points like Γ and M have a low QP weight, while on the contrary for the lines $B - B'$, $A' - A$ the QP weight is relatively high (some spectral functions can be seen in Fig. S4 in Ref. [24]).

It was claimed previously that the one-hole dispersion in T-CuO requires a three-band model to be described correctly [15]. The evidence presented came from a variational calculation on the spin-fermion model Eq. (1), whose results a one-band model supposedly cannot capture. In particular, it was shown that the minimum that the QP dispersion has at $(\pi/2, \pi/2)$ for CuO_2 (or, equivalently in T-CuO, if the two CuO_2 sublattices are disconnected), shifts along the diagonal $\Gamma \equiv (0,0) - (\pi,\pi)$, towards the Γ point, when the two CuO_2 sublattices are connected to form T-CuO. This happens for $\mathbf{Q} = (0,\pi)$. Alternatively, the shift is along the antidiagonal towards X/M for $\mathbf{Q} = (\pi, 0)$. This is what we have shown in Fig. 2. These results are in line with previous investigations for CuO_2 planes [16], where it was claimed that a one-band $t - t' - t'' - J$ model has a minimum at $(\pi/2, \pi/2)$ that along the diagonal of the Brillouin zone is controlled by spin fluctuations, while in the three-band model the variational method used in Ref. [16] does not need to include spin fluctuations in order to have an absolute minimum at $(\pi/2, \pi/2)$.

Using the generalized $t - J$ model [Eq. (2)] derived from H_{sf} [Eq. (1)], we now calculate the QP dispersion along the same path as in Ref. [15] and with the corresponding parameters (set B of Table III in Ref. [24]), and $\mathbf{Q} = (0,\pi)$. Results are shown in Fig. 4, plotted adopting the hole's picture. As before, a broadening equivalent to 20 meV was applied to the spectral functions, but the results do not depend significantly on this (unless broadenings an order of magnitude larger are applied). It is clear that, when both sublattices are connected through the t_0 term, the QP dispersion relation derived from H_{sf} is recovered. In particular, we obtain a shift of the QP minimum along the diagonal towards the Γ point, although this shift is lower (about half) in magnitude than the one obtained with the three-band model. This difference might be due to the different theoretical treatments used by Adolphs *et al.* to solve H_{sf} [Eq. (1)] and by us to solve H_{tJ} [Eq. (2)]. In this respect, we remark it is very difficult to decide which theoretical treatment gives more accurate results from quantitative differences of this kind, since on one hand both compare very well with ED results in finite clusters, while on the other hand no experiment so far could even measure this shift in the QP dispersion relation. We also remark that, by varying t_2, the QP dispersion relation is not changed apart from a constant shift (in agreement with previous results [16]). This is important, since t_2 is the parameter obtained with less accuracy.

The shift in our model is not caused by the coupling of the hole with spin fluctuations, which in fact conspires against it. This can be seen from the effective Hamiltonian Eq. (4), since the bare-hole dispersion (i.e., with no coupling to magnons) $\epsilon_{\mathbf{k}} = 2t_0 \cos(\mathbf{k}\cdot\mathbf{c}) + 4t_2 \cos(ak_x)\cos(ak_y) + 2t_3[\cos(2ak_x) + \cos(2ak_y)]$ has a minimum, along the diagonal $k_x = k_y$, that shifts from $(\pi/2, \pi/2)$ towards the Γ point when the intersublattice hopping t_0 is turned on. For example, the bare hole minimum is at $(0.4\pi, 0.4\pi)$ for the parameter set we used. However, when the interaction of the bare hole with spin fluctuations (magnons) is taken into account through the vertex M_{kq}, the minimum shifts back towards $(\pi/2, \pi/2)$. The shift obtained is about 10% of the distance between the A and Γ points. Note that the SCBA contains an infinite number of spin fluctuations, while only a few are included in the treatment in Ref. [15]. In any case, we have shown that a ZR one-band model can explain a shift in the QP minimum at $(\pi/2, \pi/2)$ and that the interaction of the bare hole with spin fluctuations is not responsible for this shift.

Finally, the QP bandwidth along this path is, in our one-band model, of the order of $3J$, slightly less than the result from the variational method in the three-band model Eq. (1) [15].

Overall, we conclude that our effective generalized one-band model, rigorously derived from orthogonalized ZR singlets, and without free parameters, not only does recover characteristics of the three-band model, but also its predictions agree qualitatively and quantitatively with ARPES experiments in tetragonal CuO.

We thank A. Greco for fruitful discussions. I. J. H. was partially supported by PICT 2014-3290 of the ANPCyT. I. J. H. and L. O. M. are partially supported by PIP 0364 of CONICET. A. A. A. is sponsored by PIP 112-201101-00832 of CONICET and PICT 2013-1045 of the ANPCyT.

*aligia@cab.cnea.gov.ar

[1] N. Nücker, H. Romberg, X. X. Xi, J. Fink, B. Gegenheimer, and Z. X. Zhao, Phys. Rev. B **39**, 6619 (1989).
[2] M. Takigawa, P. C. Hammel, R. H. Heffner, Z. Fisk, K. C. Ott, and J. D. Thompson, Phys. Rev. Lett. **63**, 1865 (1989).
[3] M. Oda, C. Manabe, and M. Ido, Phys. Rev. B **53**, 2253 (1996).
[4] F. C. Zhang and T. M. Rice, Phys. Rev. B **37**, 3759 (1988).
[5] L. F. Feiner, J. H. Jefferson, and R. Raimondi, Phys. Rev. Lett. **76**, 4939 (1996), and references therein; A. A. Aligia, F. Lema, M. E. Simon, and C. D. Batista, Phys. Rev. Lett. **79**, 3793 (1997); L. F. Feiner, J. H. Jefferson, and R. Raimondi, Phys. Rev. Lett. **79**, 3794 (1997).
[6] V. J. Emery and G. Reiter, Phys. Rev. B **38**, 11938 (1988).
[7] F. C. Zhang, Phys. Rev. B **39**, 7375 (1989).
[8] H. Q. Ding, G. H. Lang, and W. A. Goddard, III, Phys. Rev. B **46**, 14317 (1992).
[9] C. D. Batista and A. A. Aligia, Phys. Rev. B **48**, 4212 (1993); **49**, 6436(E) (1994).
[10] A. A. Aligia, M. E. Simon, and C. D. Batista, Phys. Rev. B **49**, 13061 (1994), and references therein.
[11] H. Yamase, M. Bejas, and A. Greco, Europhys. Lett. **111**, 57005 (2015).
[12] M. Bejas, A. Greco, and H. Yamase, Phys. Rev. B **86**, 224509 (2012).
[13] A. Greco, Phys. Rev. Lett. **103**, 217001 (2009).
[14] A. Chainani, M. Sicot, Y. Fagot-Revurat, G. Vasseur, J. Granet, B. Kierren, L. Moreau, M. Oura, A. Yamamoto, Y. Tokura, and D. Malterre, Phys. Rev. Lett. **119**, 057001 (2017).
[15] C. P. J. Adolphs, S. Moser, G. A. Sawatzky, and M. Berciu, Phys. Rev. Lett. **116**, 087002 (2016).
[16] H. Ebrahimnejad, G. A. Sawatzky, and M. Berciu, J. Phys. Condens. Matter **28**, 105603 (2016).
[17] V. J. Emery, Phys. Rev. Lett. **58**, 2794 (1987).
[18] C. M. Varma, S. Schmitt Rink, and E. Abrahams, Solid State Commun. **62**, 681 (1987).
[19] W. Siemons, G. Koster, D. H. A. Blank, R. H. Hammond, T. H. Geballe, and M. R. Beasley, Phys. Rev. B **79**, 195122 (2009); D. Samal, H. Tan, Y. Takamura, W. Siemons, J. Verbeeck, G. Van Tendeloo, E. Arenholz, C. A. Jenkins, G. Rijnders, and G. Koster, Europhys. Lett. **105**, 17003 (2014).
[20] S. Moser, L. Moreschini, H.-Y. Yang, D. Innocenti, F. Fuchs, N. H. Hansen, Y. J. Chang, K. S. Kim, A. L. Walter, A. Bostwick, E. Rotenberg, F. Mila, and M. Grioni, Phys. Rev. Lett. **113**, 187001 (2014).
[21] M. S. Hybertsen, M. Schlüter, and N. E. Christensen, Phys. Rev. B **39**, 9028 (1989).
[22] C. Batista and A. A. Aligia, Solid State Commun. **83**, 419 (1992).
[23] C. D. Batista and A. A. Aligia, Phys. Rev. B **47**, 8929 (1993).
[24] See Supplemental Material at http://link.aps.org/supplemental/10.1103/PhysRevLett.120.177001 for details about the derivation of the effective Hamiltonian and the SCBA, which includes Refs. [1–4,6,7,10,15,17,18,20–23,25–40].
[25] M. E. Simon, A. A. Aligia, C. D. Batista, E. R. Gagliano, and F. Lema, Phys. Rev. B **54**, R3780 (1996).
[26] J. Eroles, C. D. Batista, and A. A. Aligia, Phys. Rev. B **59**, 14092 (1999).
[27] I. J. Hamad, A. E. Trumper, and L. O. Manuel, Physica (Amsterdam) **398B**, 416 (2007).
[28] *Atomic Energy Levels*, edited by C. E. Moore (MBS, Washington, DC, 1958).
[29] W. A. Harrison, *Electronic Structure and the Properties of Solids* (Freeman, San Francisco, 1980).
[30] V. I. Belinicher, A. L. Chernyshev, and L. V. Popovich, Phys. Rev. B **50**, 13768 (1994), and references therein.
[31] L. F. Feiner, J. H. Jefferson, and R. Raimondi, Phys. Rev. B **53**, 8751 (1996), and references therein.
[32] V. I. Belinicher and A. L. Chernyshev, Phys. Rev. B **49**, 9746 (1994). There is a minor printing error in the expression of $\mu(\mathbf{R}_l)$.
[33] C. D. Batista and A. A. Aligia, Physica (Amsterdam) **264C**, 319 (1996).
[34] C. D. Batista, L. O. Manuel, H. A. Ceccatto, and A. A. Aligia, Europhys. Lett. **38**, 147 (1997).
[35] I. J. Hamad, Ph.D. thesis, Universidad Nacional de Rosario, 2009.
[36] G. Martínez and P. Horsch, Phys. Rev. B **44**, 317 (1991).
[37] F. Lema and A. A. Aligia, Phys. Rev. B **55**, 14092 (1997).
[38] F. Lema and A. A. Aligia, Physica (Amsterdam) **307C**, 307 (1998).
[39] A. E. Trumper, C. J. Gazza, and L. O. Manuel, Phys. Rev. B **69**, 184407 (2004).
[40] I. J. Hamad, A. E. Trumper, A. E. Feiguin, and L. O. Manuel, Phys. Rev. B **77**, 014410 (2008).
[41] I. J. Hamad, L. O. Manuel, and A. E. Trumper, Phys. Rev. B **85**, 024402 (2012).
[42] Note that in the exact diagonalization of the QP dispersion, unless some small anisotropy is put by hand, the two magnetic degenerate ground states coexist in the calculation, and, hence, the results should reflect this fact [40].